Impact of Physical Effects onto the Optimal Signal Power in CWDM Optical Networks

Áron Szabó, Szilárd Zsigmond, Tibor Cinkler
Budapest University of Technology and Economics/Department of Telecommunications and Media Informatics,
aron.szabo@tmit.bme.hu, zsigmond@tmit.bme.hu, cinkler@tmit.bme.hu

Abstract—**Nowadays in optical networks there is a trend to extend the maximum transmission distance. Several technical solutions are known but the simplest one is to increase the signal power in the optical fiber.**
However, the nonlinear behavior of the optical fiber limits the signal power e.g. the span of the all-optical network.
This paper presents an analytical model and calculation results for the signal quality degradation in an 8-channel and an 18-channel, 2.5 Gbps coarse wavelength-division-multiplexing (CWDM) system. Based on the proposed model and performed analysis we give the optimal value of the signal power at the transmitter point.

***Index terms*—Coarse wavelength-division-multiplexing (CWDM), dense wavelength-division-multiplexing (DWDM), Q-factor, stimulated Raman-scattering (SRS), group velocity dispersion (GVD), relative intensity noise (RIN)**

I. Introduction

Today it is becoming increasingly important to transmit data as close to the users as possible, but at a lower price, offering a convenient bit rate. It is mostly the tendency in metropolitan area networks (MANs). Coarse wavelength division multiplexing (CWDM) standard is suitable for this purpose, using the 1270 nm-1610 nm band with 20 nm channel spacing for 18 channels. In most cases only the top wavelength band is built in CWDM systems, using 8 channels from 1470 nm to 1610 nm because of the fiber's OH^- attenuation peak at 1383 nm and the lack of high-quality lasers near 1400nm.

The paper presents an analytical model and calculation results for the signal quality degradation in 8-channel and 18-channel point-to-point CWDM links due to physical effects. We used the results to determine the highest input signal level at which the signal quality remains convenient. Nonlinear effects in wavelength-division-multiplexed systems have been studied extensively, but so far there has been no study that summarizes the impacts of the significant linear and nonlinear effects in CWDM systems and derives the optimal inserted signal power in view of them.

The derived results can be used to determine the optimal inserted signal power for a point-to-point CWDM link and to give numerical values of the signal quality changed due to the physical effects.

II. The Theoretical Model

The nonlinear behavior of the DWDM systems has been investigated in [1], [2]. In the case of CWDM systems only stimulated Raman-scattering (SRS) and stimulated Brillouin-scattering (SBS) have a significant impact [2],[3]. Since most CWDM systems work at 2.5 Gbps per channel bit rate, this bit rate is assumed in the model. The polarization mode dispersion (PMD) and the polarization-dependent loss (PDL) are neglected because of the relatively low bit rate [4]. Dispersion compensation units (DCUs) are widely used in DWDM systems, but ignored in CWDM systems, consequently group velocity dispersion (GVD) is important and affects differently each channel. Beyond physical effects of propagation the model considers the transmitter's intensity noise. Amplifiers are not widespread in CWDM systems so amplifier spontaneous emission (ASE) is not involved in the model [5]. Calculations are based on the numerical data of the ITU-T G.652 optical fiber. The studied architecture is shown in Fig. °1

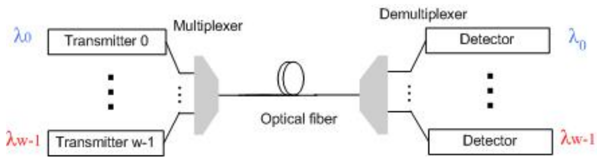

Figure 1. The studied architecture

The main goal is to calculate the impact of the physical effects on the signal quality measured at the fiber end. The signal quality is described by the Q-factor:

$$Q = \frac{\mu_1 - \mu_0}{\sigma_1 + \sigma_0} \tag{1}$$

The bit 1 and the bit 0 signal levels are assumed to be Gaussian probability variables with μ_1 and μ_0 mean values and their standard deviations are σ_1 and σ_0.

The transmitter intensity noise is calculated using the $-120 dB/Hz$ maximum relative intensity noise (RIN_{dB}) value at 0 dBm signal power, which is prevalent for CWDM transmitters [6]. A method shown in [7] is used to calculate the dimensionless noise ratio (σ) of a signal:

$$\sigma = \sqrt{B_c \cdot 10^{RIN_{dB}/10}} \tag{2}$$

where B_c is the receiver electrical bandwidth. Denoting the signal powers 1 and 0 by P_1 and P_0, taking the prevalent 7.4dB extinction ratio for P_1/P_0 at the starting point and assuming that the power dependence of the RIN

[1/Hz] is proportional to $1/P^3$ [8], the RIN-related noise of the signal levels can be readily calculated.

The discussion of the propagation-related effects includes the chromatic dispersion and the stimulated Raman-scattering. The stimulated Brillouin-scattering limits the inserted power, and the Brillouin power thresholds can be calculated. Since many technologies exist to increase the Brillouin threshold thus present calculation is executed both, below and over the calculated Brillouin thresholds.

A. The chromatic dispersion (CD)

There is no modal dispersion in G.652 fibers because they are single mode fibers. Consequently the D dispersion parameter of the fiber is calculated as the sum of the material dispersion parameter and the waveguide dispersion parameter.

At the ending point of the fiber the signal is sampled at the half of the bit period. The chromatic dispersion changes the original signal shape, therefore the sampled signal level differs from the maximum of the level inserted into the fiber at the starting point.

The change of the signal shape is calculated using the equations shown in [1]:

$$U(z,T) = \frac{1}{2\pi}\int_{-\infty}^{\infty}\widetilde{U}(0,\omega)\exp\left(\frac{i}{2}\beta_2(\omega)\omega^2 z - i\omega T\right)d\omega \quad (3)$$

where

$$U(z,T) = \left(1/\sqrt{P}\right)\exp(\alpha z/2)A(z,T) \quad (4)$$

is the attenuation-normalized amplitude, z is the distance from the starting point of the fiber,

$$T = t - z/v_g \quad (5)$$

is the reduced time using the group velocity v_g, P is the power inserted into the investigated channel, α is the attenuation,

$$\widetilde{U}(0,\omega) = \int_{-\infty}^{\infty}U(0,T)\exp(i\omega T)dT \quad (6)$$

is the Fourier-transform of the inserted signal at $z = 0$. $\beta_2(\omega)$, which is the second term in the Taylor series of the mode propagation constant, is calculated using the disclosed $D(\lambda)$ dispersion parameter of the ITU-T G.652 fiber [9].

For further calculations the knowledge of the $U(z,T)$ signal shape is required. For directly modulated semiconductor lasers the signal shape is well approximated by the super-Gaussian function [1]:

$$U(0,T) = \exp\left[-\frac{1+iC}{2}\left(\frac{T}{T_0}\right)^{2m}\right] \quad (7)$$

where T_0 is the half-width at the $1/e$ intensity point, C is the chirp parameter characterizing the spectral power density of the laser and the m parameter controls the degree of the pulse edge sharpness. Using disclosed transmitter data [10], a realistic estimation is $m = 3$. In our calculation we use a typical value of $C = -3.6$ [11]. We suppose that the chirp parameter is independent of the modulation frequency and the intensity [12].

For both bit 0 and bit 1 signals we performed the calculation in the cases of each possible adjacent bit, assuming these bit sequences to have the same probability. In the case of bit 1, the 010, 011, 110, 111 sequences are investigated and they have one by one ¼ probabilities, similarly in the case of bit 0, the 000, 001, 100, 101 sequences are investigated and have also one by one ¼ probabilities. Simulating non-return-to-zero (NRZ) modulation, the chromatic dispersion related μ_{1CD} and μ_{0CD} mean values are calculated at the ending point of the fiber. In our model we use the previously released approximation [13] that the chromatic dispersion affects the mean values but leaves the standard deviations invariably, equation (1).

B. The stimulated Raman-scattering (SRS)

Stimulated Raman-scattering is an inelastic scattering process in which higher energy photons of the pump wave scatter on the medium molecules producing lower energy photons and optical phonons. The beam containing the lower energy photons is called the Stokes wave. If there are photons at the lower energy state, SRS becomes an amplification process that occurs where the bit 1 signal of the pump wave overlaps the bit 1 signal of the Stokes wave. This way energy is transmitted from the higher energy channels into the lower energy ones. In the case of SRS the Stokes waves have the same direction as the pump waves therefore the Stokes waves produce a noise in the pump waves.

Investigating the interaction of only 2 channels with narrow channel spacing, the interaction of the pump and the Stokes wave has already been studied in [14]. This model supposes narrow channel spacing and is ideal for DWDM calculations, where the channel spacing is approximately 1nm. This model must be modified in the case of CWDM systems because of the 20nm channel spacing. The model includes a $g_R'\Delta f_{ji}$ factor where i denotes the number of a pump channel and j denotes the number of a Stokes channel, Δf_{ji} is the frequency difference between the pump and the Stokes wave, g_R' is the Raman-gain slope, which is the derivative of the Raman-gain spectrum near $\Delta\omega_{ji} = 0$.

In the case of CWDM systems, the $g_R'\Delta f_{ji}$ factor must be replaced by $g_R(j,i)$ defined by the gain spectrum shown in Fig. 2.

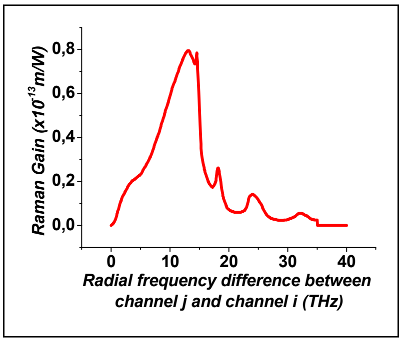

Figure 2 The Raman gain spectrum

Furthermore, a Raman-gain value is inversely proportional to the pump wavelength [1].

In [14], the depletion of the pump channel caused by the SRS is characterized by a Gaussian probability variable $x(z,t)$, where z and t denote the distance from the starting point of the fiber and the time.

Approximating the waveforms by NRZ-modulated rectangular shapes, the deviation and the mean value of $x(z,t)$ denoted by σ_x and μ_x can be calculated [14]. In this case, z equals to the fiber length.

In the current many-channel case we used the approximation that the interaction of the channels can be discussed by each possible combination of pairs of pump waves and Stokes-waves. In this case, σ_x and μ_x are replaced by σ_{xji} and μ_{xji} representing the interaction of channel j and channel i. For a given channel i we summarized the impact of all the other channels to determine the evolution of the power in channel i:

$$\mu_{xi} = \sum_{\substack{j=1\\j\neq i}}^{W} \mu_{xji} - \sum_{\substack{j=1\\j\neq i}}^{W} \mu_{xij} \qquad (8)$$

$$\sigma_{xi}^2 = \sum_{\substack{j=1\\j\neq i}}^{W} \sigma_{xji}^2 + \sum_{\substack{j=1\\j\neq i}}^{W} \sigma_{xij}^2 \qquad (9)$$

where W is the number of the channels. We assume that each impact can be described by independent probability variables; equation (9). Using (8) and (9), the real effect of SRS on the signal level and noise, μ_{1SRS} and σ_{1SRS} respectively, can be calculated [14].

C. Calculating the Q-factor

Q-factors are calculated one by one for each channel to describe the total impact of the CD, the RIN and the SRS at given fiber lengths as functions of the inserted power. They are calculated using the approximation that the CD and the SRS act independently. In our model, the same signal power was inserted into each channel. The attenuation is taken into account by a multiplication with $e^{-\alpha L}$, where α and L denote the attenuation and the fiber length.

As it can be seen by the next equations, in this model the attenuation has no effect on the Q-factor, but irrespectively of this the receiver sensitivity limits the minimum received power.

$$Q_{tot} = \frac{\mu_{1SRS}\mu_{1DISP}e^{-\alpha L} - \mu_{0DISP}e^{-\alpha L}}{\sqrt{\sigma_{1RIN}^2 + \sigma_{1SRS}^2}\, e^{-\alpha L} + \sigma_{0RIN}e^{-\alpha L}} = \frac{\mu_{1SRS}\mu_{1DISP} - \mu_{0DISP}}{\sqrt{\sigma_{1RIN}^2 + \sigma_{1SRS}^2} + \sigma_{0RIN}} \qquad (10)$$

Furthermore we define the Q_{SRS} to describe the effect of SRS alone on the signal quality:

$$Q_{SRS} = \frac{\mu_{1SRS}}{\sigma_{1SRS}} \qquad (11)$$

and similarly

$$Q_{CD,RIN} = \frac{\mu_{1CD} - \mu_{0CD}}{\sigma_{1RIN} + \sigma_{0RIN}} \qquad (12)$$

In (11) we used that the SRS has no effect on the signal level 0.

III. CALCULATION RESULTS

In this section we present the calculation results for the Q factors of the 8-channel CWDM systems that uses the upper CWDM wavelength band and also for 18-channel systems that uses the whole band. We performed the calculations for different fiber lengths and present the Q factor values of each channel as a function of the inserted power.

We assume that the signal quality remains convenient if the Q factor deteriorated by the studied physical effects is over 14 for each channel. Using this assumption, the maximum inserted power for a given system configuration is defined as the highest inserted power at which $Q \geq 14$ for each channel. The channel for which Q=14 at this power is called the most power-sensitive channel. Table I summarizes the main parameters of the optical system used for the calculations.

TABLE I
THE MAIN PARAMETERS OF THE OPTICAL SYSTEM

Bit rate	2.5Gbps
Wavelength band of the 8-channel CWDM system	$1470nm - 1610nm$
Wavelength band of the 18-channel CWDM system	$1270nm - 1610nm$
Channel spacing	$20nm$
Speed of light in vacuum	299792458 m/s
Effective core area	$80\mu m^2$
Maximum RIN at 0 dBm	$-120dB/Hz$
Optical bandwidth of the receiver	$10GHz$
Electrical bandwidth of the receiver (B_e)	$1.75GHz$
Fiber length (L)	$60km,\ 100km,\ 140km$
Chirp parameter of the transmitter (C)	-3.6
Super-Gaussian edge sharpness parameter (m)	3
Extinction ratio (P_1/P_0)	7.4 dB
Dispersion parameter $D(\lambda)$	Fiber specification [9]
Raman gain (g_R)	Fig. °2

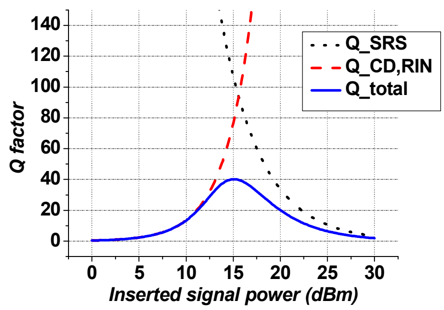

Figure 3. Q factor dependency from chromatic dispersion, relative intensity noise and Raman scattering

Fig. 3 shows the general behavior of $Q_{CD,RIN}$, Q_{SRS} and Q_{tot} as functions of the inserted power. The example shows the Q factor values of the 1470nm channel in the 8-channel system with 140km fiber length. As it can be clearly seen, increasing the inserted power produces increasing $Q_{CD,RIN}$, because the proportion of the RIN to $1/P^3$ produces decreasing σ_{1RIN} and σ_{0RIN}, while the effect of the chromatic dispersion does not depend on the inserted power but it is a function of the fiber length and the wavelength of the channel. However, if the inserted power is high enough, the effect of SRS becomes significant and deteriorates the signal quality, therefore Q_{SRS} decreases. At lower inserted powers, the effect of SRS is negligible, but the high noise rate induced by the high RIN produces a low Q factor value. Taken all round, a maximum value of the Q factor at a given power exists for each channel in each system configuration.

Fig. 4 shows the power-dependence of the Q factors calculated for each channel in 8-channel and 18-channel systems with 60km, 100km and 140km fiber length. We show the Q factor values of 3 channels in the case of the 8-channel systems and the Q factor values of 4 channels in the case of the 18-channel systems including the most power-sensitive channel in each case.

In the case of the 8-channel systems the most power-sensitive channel has a relatively low wavelength. The inserted powers that belong to the maximum values of the Q factors for different channels are changing even for the same fiber length, but they are all near 15dBm. This aberration is caused by the wavelength dependence of the CD and the SRS.

In the 18-channel case the wavelength of the most power-sensitive channel is in the medium wavelength domain in contrast to the 8-channel case. The power values that belong to the maximum Q factors of different channels differ for the same fiber length in this case too, but the power values are on average higher than in the 8-channel case, they are near 20dBm.

We defined the optimal signal power to be the highest power at which $Q \geq 14$ for each channel. Table II shows these power values both for the 8-channel and the 18-channel systems.

TABLE II
THE OPTIMAL SIGNAL POWER VALUES FOR THE 8-CHANNEL AND THE 18-CHANNEL SYSTEM WITH DIFFERENT FIBER LENGTHS $(Q \geq 14)$

	60km	100km	140km
8 channels	21.2dBm	20.0dBm	21.0dBm
18 channels	25.3dBm	25.1dBm	26.3dBm

The optimal power values of the 18-channel system are appreciably higher than those of the 8-channel system, which is a direct consequence of the higher channel number. The optimal power values do not increase linearly with the channel number because of the increasing intra-channel interaction.

Finally, we can answer a question: "Can a signal be better after 140 km than after 100 km?" Yes, it can, as it is clearly seen by Fig. 4 and by Table II. The Q factor values and the optimal signal powers are higher after 140km than after 100km in both the 8-channal and the 18-channel case.

The key is the dispersion of the super-Gaussian signal shape. This shape not only broadens but produces peaks and valleys because of the CD [15]. For appropriate fiber lengths, e.g. 140km, a dispersion-induced peak arrives at the ending point of the fiber, enhancing the Q factor considerably.

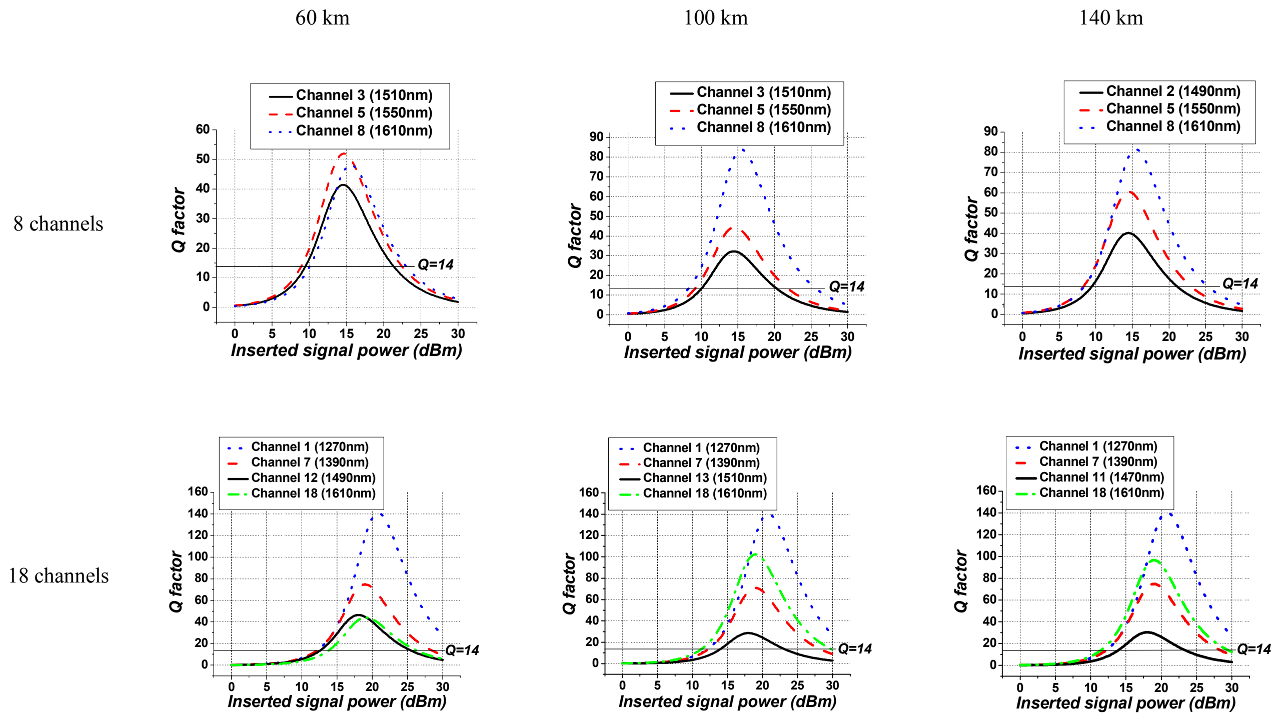

Figure 4. Input power dependence of the Q factor in an 8-channel and in an 18-channel system with 60km, 100km, and 140km fiber length

IV. CONCLUSION

In this paper we presented the dependence of the physical effects and the signal quality on the signal power and the fiber length for 2.5Gbps CWDM systems. We show by analytical calculations which are the optimal signal powers for different network scenarios. These results are useful tools for network designers for improving their optical network or even redesigning their power budget calculations.

REFERENCES

[1] Govind P. Agrawal, “Nonlinear Fiber Optics”, 3rd edition, Academic Press, 2001

[2] VPI Transmission Maker User’s Manual, VPI Photonics, 1996-2007; http://www.vpiphotonics.com/

[3] Adding/Splitting Nodes With Limited Glass Using CWDM Technologies; Central FL SCTE Chapter Presentation Nov 1, 2006

[4] Vivek Alwayn, “Fiber-Optic Technologies”, Pearson Education, Cisco Press, 2004; http://www.ciscopress.com/

[5] W. Shin, I. B. Sohn, B.-A. Yu, Y. L. Lee, S. C. Choi, Y.-C. Noh, J. Lee, D.-K. Ko, „Microstructured Fiber End Surface Grating for Coarse WDM Signal Monitroing”, IEEE Photonics Technology Letters, Vol. 19, No. 8, April 15, 2007

[6] Finisar Product Specification: Multi-rate CWDM Pluggable SFP Transceiver, FWDM-1621-7D-xx; Finisar Corporation September 2005 Rev. F

[7] „Impact of Transmitter RIN on Optical Link Performance”, Maxim High- Frequency/Fiber Communications Group; Application Note: HFAN-9.1.0 Rev 0; 10/04

[8] L. A. Coldren and S. W. Corzine, “Diode Lasers and Photonic Integrated Circuits”, New York: Wiley, 1995.

[9] Drew Perkins “Dispersion and Skew” IEEE HSSG Interim; September 20, 2006

[10] Appointech INC – 2,5Gbps CWDM laser diode modul, 2005-10, http://www.appointech.com/downloads.html

[11] Aragon Photonics Labs Whitepaper (WP001_0100_0307), 2007; http://www.aragonphotonics.com/docs/gc_fichas/doc/56FIPSprxy.pdf

[12] A. Villafranca, et al. „Linewidth Enhancement Factor of Semicondutor Lasers: Results from Round-Robin Measurements in COST 288” in CLEO07, Baltimore, USA. May 2007

[13] Bing Xie, Yong Liang Guan, Jian Chen and Chao Lu **“**Improvement of dispersion tolerance using wavelength-interleaving and forward error correction”. IEEE School, Nanyang Technological University, Singapore; 10 July 2006

[14] Keang Po Ho “Statistical Properties of Stimulated Raman Crosstalk in WDM Systems”, pp. 915-921; Journal of Lightwave Technology, VOL.18, NO. 7, JULY 2000

[15] Guangqiong Xia, Zhengmao Wu, Jianwei Wu “Effect of Fiber Chromatic Dispersion on Incident Super-Gaussian Pulse Transmission in Single-Mode Fibers” pp. 116-120, July 8, 2005